Photodissociation dynamics of 3-cyclopentenone: using the impact parameter distribution as a criterion for concertedness

ARTICLE *in* CHEMINFORM · MAY 1992

Impact Factor: 0.74 · DOI: 10.1021/j100190a018

6 AUTHORS, INCLUDING:

Ralph Jimenez
University of Colorado Boulder
89 PUBLICATIONS **3,394** CITATIONS

SEE PROFILE

Scott H Kable
University of New South Wales
148 PUBLICATIONS **2,288** CITATIONS

SEE PROFILE

Jean-Christophe Loison
Institut des Sciences Moléculaires
80 PUBLICATIONS **978** CITATIONS

SEE PROFILE

ARTICLES

Photodissociation Dynamics of 3-Cyclopentenone: Using the Impact Parameter Distribution as a Criterion for Concertedness

R. Jimenez,[†] S. H. Kable,[‡] J-C. Loison,[§] C. J. S. M. Simpson,[⊥] W. Adam,[∥] and P. L. Houston*

Department of Chemistry, Cornell University, Ithaca, New York 14853-1301 *(Received: October 7, 1991; In Final Form: January 21, 1992)*

The cyclic ketone 3-cyclopentenone has been dissociated in a molecular beam with a pulsed excimer laser to yield butadiene and CO, and the CO product state distribution has been measured using vacuum ultraviolet laser-induced fluorescence with full rovibronic state resolution. It is found that the CO rotational temperatures in $v = 0$ and 1 are 3500 ± 140 and 7500 ± 400 K, respectively, and that the vibrational distribution is characterized by a temperature of 1750 ± 200 K. It is also observed from Doppler profile measurements that the average translational energy of the CO fragment increases with J in the range $J = 0$–60, contrary to what would be expected on a statistical basis, that the CO recoils isotropically in the laboratory frame, and that the CO is produced with its rotation vector predominantly perpendicular to its velocity vector. Comparison with a simple prior model shows that the CO product has the statistically expected rotational distribution in $v = 0$ but is much hotter than expected in $v = 1$. The CO vibrational distribution is also much colder than expected on a statistical basis. The maximum entropy formalism is used to calculate an impact parameter distribution from the data. Comparison of the prior impact parameter distribution to that calculated from the data shows that the dissociation takes place through a restricted region of the phase space available to the system. Physical interpretation of this impact parameter distribution strongly suggests that the reaction occurs in a concerted manner, with both C–C bonds breaking simultaneously as the CO bends out of the cyclopentenone plane, so that v and J for CO are perpendicular. Conservation of angular momentum suggests that a fixed distribution of impact parameters is responsible for the increase of velocity with rotational quantum number.

Introduction

While great advances have been made in elucidating the dissociation dynamics of small molecules, the majority of investigations of larger molecules have simply determined product yields either in solution or in high-pressure bulb experiments.[1,2] It is clear that our understanding of the dissociation of these larger systems could benefit from studies undertaken with state resolution and collision-free conditions. What are the nascent product distributions, and what is the mechanism of dissociation? If more than one bond breaks, what is the order of cleavage? Consider in general terms a few systems in which two bonds are broken to produce a diatomic fragment.

Even since it was pointed out by Bauer[3] that large changes take place between the CO or NN bond lengths in organic molecules and those in the free diatomic molecules, there has been speculation as to whether the concerted dissociation of carbonyls and azo compounds would lead to highly vibrationally excited CO and N_2 products. Since the N=N bond lies perpendicular to the reaction coordinate, the azo compounds might be particularly favorable cases for the production of vibrationally excited N_2 molecules. However, using a combination of direct experiments and RRKM calculations, Dougherty and co-workers[4] established that in the thermolysis the N_2 is born with very little vibrational energy following the dissociation

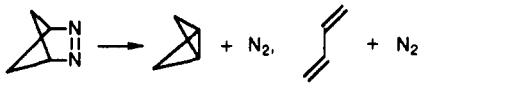

The same conclusion has been reached from a shock tube study[5] of the thermal dissociation:

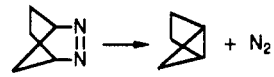

Early mechanistic studies based on product analysis suggested that $\pi^* \leftarrow n$ excitation of cyclic azoalkanes denitrogenate in a stepwise fashion by way of diazyl diradicals.[6] A similar conclusion for the photochemical investigation was made by using CARS spectroscopy to detect the nascent vibrational and rotational state of the N_2.[7] The authors concluded that the cyclic azo compound dissociates via a diazenyl biradical mechanism and does not yield vibrationally excited N_2. It is surprising that Weisman and co-workers also found the N_2 to be rotationally cold as well as vibrationall cold, since one would expect rotational excitation to result from asynchronous bond rupture.

The carbonyl compounds have the experimental advantage that the nascent vibrational state of the CO can be monitored following thermal shock tube decomposition by using a continuous wave CO laser. This technique can never give information on the nascent rotational distribution of the CO, however, since fewer collisions are needed to relax rotationally the CO than to dissociate the parent molecule. Far more information can be obtained using

[†] Current address: The University of Chicago, Department of Chemistry, 5735 S. Ellis Ave., Chicago, IL 60637.
[‡] Current address: Department of Physical & Theoretical Chemistry, University of Sydney, Sydney, 2006, Australia.
[§] Current address: Laboratoire de Photophysique Moléculaire, Bâtiement 213, Université de Paris-Sud, Orsay Cedex F-91405, France.
[⊥] Permanent address: Physical Chemistry Laboratory, South Parks Road, Oxford, OX1 3QZ, UK.
[∥] Institute of Organic Chemistry, University of Würzburg D-8700 Würzburg/Hubland, Germany.
* To whom correspondence should be addressed.

(1) Wentrup, C. *Reactive Molecules*; John Wiley and Sons: New York, 1984.
(2) Engel, P. S. *Chem. Rev.* **1980**, *80*, 99.
(3) Bauer, S. H. *J. Am. Chem. Soc.* **1969**, *91*, 3688.
(4) Chang, M. H.; Jain, R.; Dougherty, D. A. *J. Am. Chem. Soc.* **1984**, *106*, 4211.
(5) Simpson, C. J. S. M.; Wilson, G. J.; Adam, W. *J. Am. Chem. Soc.* **1991**, *113*, 4728.
(6) Adam, W.; Carballeira, N.; Gillaspey, W. D. *Tetrahedron Lett.* **1983**, *24*, 5473. Adam, W.; Gillaspey, W. D.; Peters, E.-M.; Peters, K.; Rosenthal, R. J.; von Schnering, H. G. *J. Org. Chem.* **1985**, *50*, 580, 587. Adam, W.; Oppenländer, T.; Zang, G. *J. Org. Chem.* **1985**, *50*, 3303. Adam, W.; De Lucchi, O.; Dörr, M. *J. Am. Chem. Soc.* **1989**, *111*, 5209. Adam, W.; Zhang, G. *J. Org. Chem.* **1991**, *56*, 3315.
(7) Adams, J. S.; Engel, P. S.; Weisman, R. B. *J. Am. Chem. Soc.* **1990**, *112*, 9115.

0022-3654/92/2096-4188$03.00/0

photochemical dissociation and a pulsed, tunable vacuum ultraviolet (VUV) laser to probe the CO by laser-induced fluorescence (LIF).

The thermal decompositions of the cyclic compounds **1–8** have been investigated by Simpson and co-workers using a shock tube and a cw CO laser.[8] Compound **1** polymerizes readily. Compound **2** gives a variety of products. Compound **3** fragments cleanly to give 1,3-butadiene and CO. The CO is born with less than its statistical share of the energy released in vibration. Compounds **4**, **5**, and **8** give CO with its statistical share of energy. These probably fragment via biradical paths and have considerably higher activation energies for this dissociation than compounds **3**, **6**, and **7**, for which concerted dissociation is orbitally allowed.[9] It is interesting that while the CO from compounds **3** and **7** is born with less than its statistical share of the energy released in vibration, compound **6** has its statistical share. The molecular dynamics of the dissociation must be controlling the state of the CO produced for the dissociation of compounds **3** and **7**, and an explanation is needed as to why compound **6** behaves differently. Buxton and Simpson have pointed out one difference between the dissociations; in the latter case the bond cleavage is accompanied by conrotary motion of the orbitals, while in the former the motion is disrotary.[10] An investigation of the photolysis under collision free conditions using a tunable VUV-LIF to measure the rotational, vibrational, and Doppler profiles of the CO might elucidate the molecular dynamics involved.

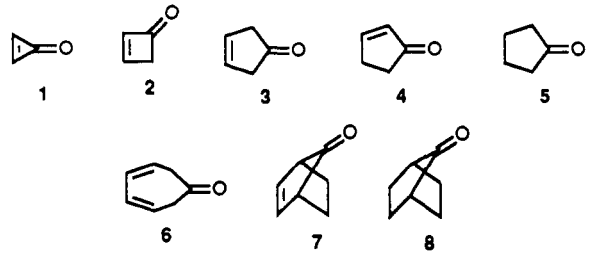

The thermal decomposition of 3-cyclopentenone (3-CPE, compound **3**) was studied between 598 and 653 K by Dolbier and Frey.[11] They found only CO and 1,3-butadiene (BDE) to be formed. Since they estimated the energy of activation for the formation of the biradical to be 253 kJ/mol and measured the activation energy to be 214.4 ± 0.8 kJ/mol, they concluded that the dissociation occurs by a concerted process, allowed by the Woodward–Hoffmann rules.[9]

The photochemical decomposition was first studied by Hess and Pitts, who used gas chromatography to analyze the products.[12] They found that excitation of the singlet–singlet $\pi^* \leftarrow$ n transition at 313 nm gives only CO and 1,3-butadiene with nearly unit quantum yield.

Using a gas cell and a continuous-wave CO laser, Rosenfeld and co-workers measured the nascent vibrational distribution of the CO following photolysis of 3-CPE by using excimer laser lines at 193, 248, and 308 nm.[13,14] CO vibrational temperatures of 2900, 1800, and 640 K were found, respectively, at these wavelengths. These authors suggested that nonradiative decay to the ground state occurred to give highly vibrationally excited parent molecules prior to their dissociation. However, the experiments were not performed under collisionless conditions. Indeed, the lifetime of the vibrationally excited CO was observed to be just greater than the response time of their detection system, and vibrational relaxation of the CO was clearly observed. The measured distribution was compared to a vibrational distribution calculated by assuming that all the energy above the barrier ($E_{avail} - E_{act}$) is partitioned statistically into product vibration, where E_{act} is the activation energy for the thermal dissociation, E_{avail} is equal to $h\nu - \Delta H$, ΔH is the enthalpy change for the endothermic reaction (estimated to be 82 ± 10 kJ/mol),[5] and $h\nu$ is the absorbed laser energy (corresponding to one 193-nm photon, 619 kJ/mol). From Figure 1 we see that the energy to be shared statistically is $h\nu - E_{act}$. They measured vibrational but not rotational distributions, and full agreement was found between their measurements and their calculated vibrational distributions. More recently, Prather and Rosenfeld have measured the rotational and translational distributions as well using a tunable diode laser, also in a cell.[15] Their rotational and translational distributions also agree with their previous statistical model.

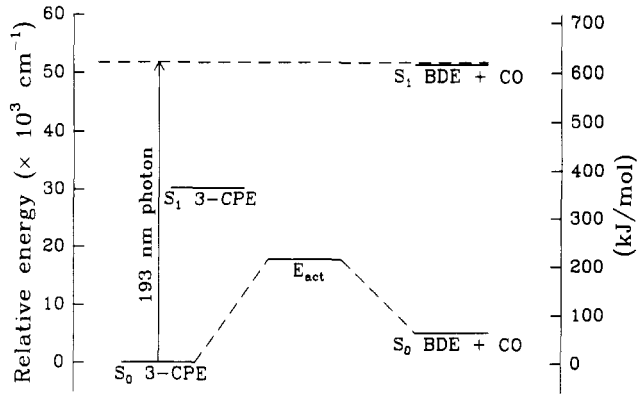

Figure 1. Energy level scheme for 193-nm decarbonylation of 3-cyclopentenone. S_1 has electronic origin at 30 248 cm^{-1}.[55] The ΔH for the process is 6900 cm^{-1}. DBE stands for butadiene.

Greater insight into the dynamics of the dissociation can be obtained from collisionless photochemical experiments in which the nascent vibrational, rotational, and translational distributions, as well as vector correlations are measured. Some important issues to address with regard to this dissociation include the degree of energy randomization among the products, the geometry of the transition state, and whether the reaction proceeds via a concerted or stepwise mechanism. In the present work, we measure the CO internal and translational energy distributions following the 193-nm photodissociation of 3-cyclopentenone. A mechanism consistent with the results is proposed based on an interpretation of the impact parameter distribution for the reaction.

Experimental Section

3-Cyclopentenone was produced using the synthesis of Hess and Brown[16] or from the epoxide using a palladium(0) catalyst[17] and stored at −30 °C. NMR analysis of the freshly prepared samples showed no detectable impurities. The samples slowly isomerized even when kept refrigerated. However, they could be repurified by vacuum distillation. The older samples gave the same results upon photodissociation as the very pure samples. Before the experiment, 3-CPE was subjected to a freeze–pump–thaw cycle in order to remove dissolved gaseous impurities. Helium at 2 atm was allowed to flow over room-temperature 3-CPE to introduce the sample into the reaction chamber as a supersonic expansion. The beam valve had an orifice of 500 μm and was operated at 10 Hz with an open pulse duration of 200 μs. The pressure in the molecular beam chamber was 2×10^{-4} Torr with the beam valve operating.

The photolysis source was an ArF excimer laser (Lambda Physik EMG101) which produced light at 193 nm. The beam was directed straight into the molecular beam chamber, generally unfocused. For Doppler measurements of weak CO lines, the 193-nm beam was loosely focused with a 40-cm cylindrical lens.

(8) Simpson, C. J. S. M.; Price, J.; Holmes, G.; Adam, W.; Martin, H.-D.; Bish, S. *J. Am. Chem. Soc.* **1990**, *112*, 5089.
(9) Woodward, R. B.; Hoffman, R. *The Conservation of Orbital Symmetry*; Verlag Chemie Academic Press: Weinheim, Germany, 1971.
(10) Buxton, J. P.; Simpson, C. J. S. M. *Chem. Phys.* **1986**, *105*, 307.
(11) Dolbier, W. R.; Frey, H. M. *J. Chem. Soc., Perkin Trans. 2* **1974**, 1674.
(12) Hess, L. D.; Pitts, J. N. *J. Am. Chem. Soc.* **1967**, *89*, 1973.
(13) Sonobe, B. I.; Fletcher, T. R.; Rosenfeld, R. N. *Chem. Phys. Lett.* **1984**, *105*, 322.
(14) Sonobe, B. I.; Fletcher, T. R.; Rosenfeld, R. N. *J. Am. Chem. Soc.* **1984**, *106*, 4352.
(15) Prather, K. A.; Rosenfeld, R. N. *J. Phys. Chem.* **1991**, *95*, 6544.
(16) Hess, H. M.; Brown, H. C. *J. Org. Chem.* **1967**, *32*, 4138.
(17) Suzuki, M.; Oda, Y.; Noyori, R. *J. Am. Chem. Soc.* **1979**, *101*, 1623.

The average laser power was about 50 mJ/pulse in the approximately 4 cm^2 region of its intersection with the free jet expansion.

CO fragments from the 193-nm photolysis of 3-CPE were detected by using the vacuum ultraviolet laser-induced fluorescence (VUV-LIF) apparatus described previously.[18] Briefly, tunable VUV radiation in the region from 140 to 170 nm was generated by four-wave sum frequency mixing of two visible dye lasers in Mg vapor. One dye laser (ω_1) was tuned to a two-photon resonant transition in the magnesium and the other (ω_2) was tuned through a continuum of autoionizing states, which produced a coherent beam at the sum frequency $2\omega_1 + \omega_2$. The photolysis and probe lasers were propagated at right angles to each other and perpendicular to the direction of the molecular beam.

Laser-induced fluorescence was collected with a solar blind photomultiplier tube (EMI G26E31LF), fitted with a 193-nm filter to reduce interference due to scattered light from the pump laser. The probe laser was delayed by 100–200 ns with respect to the photolysis laser to discriminate further against the 193-nm radiation. The fluorescence signal was processed by a gated integrator/boxcar averager (SRS250) and transferred to a microcomputer-controlled data acquisition system (DEC PDP-11) which also scanned the wavelength of the VUV probe laser. Scans were normalized to both the VUV power (detected by a second solar-blind PMT) and the photolysis laser power (detected by reflecting a small portion of the beam onto a dye cuvette containing rhodamine 6G dye and by monitoring the dye fluorescence with a photodiode). The signal was found to vary linearly with laser power, which indicated a single-photon process.

For Doppler profile measurements, etalons were inserted into both dye lasers used for VUV generation. The VUV bandwidth was thus reduced from approximately 0.6 to 0.18 cm^{-1}. The ω_2 dye laser was pressure tuned with N_2, also under microcomputer control. Multiple scans (2–4) of each transition were summed to improve the signal-to-noise ratio of the Doppler profiles. In addition, a stack of six quartz plates at the Brewster angle was used to polarize the ArF laser.

Results

The CO product vibrational and rotational state distributions have been measured by laser-induced fluorescence spectroscopy following the 193-nm photodissociation of 3-CPE. Sub-Doppler-resolved single rovibronic lines provide the CO translational energy distribution as a function of v and J, as well as dynamic information concerning the anisotropy of the photofragment recoil velocities and correlations between vector (velocity and angular momentum) and scalar (rotational, vibrational, and translational energy) properties of the CO photoproduct.

(A) CO Rotational Distributions. The LIF spectra of the CO $A^1\Pi \leftarrow X^1\Sigma^+$ 0–0 and 0–1 bands were measured. These bands determine the rotational distributions in CO $v = 0$ and 1, respectively. Values of the rovibronic levels of the perturbed $A^1\Pi$ state tabulated by Field and co-workers were used to assign the spectra completely.[19] The intensity of each rovibronic line was measured, divided by the appropriate Hönl–London factor, multiplied by its rotational degeneracy, and corrected for perturbations by the use of Field's data. A Boltzmann plot (ln [population/degeneracy] vs energy) was made to determine the suitability of representing the data by a thermal distribution. As shown in Figure 2, the data seem to be well represented by a thermal distribution with $T_{rot}(v=0) = 3500 \pm 140$ K and $T_{rot}(v=1) = 7500 \pm 400$ K. A small additional population component is evident at low J values, but it seems unlikely from the pressures and time delays that this component can be caused by rotational relaxation. The scatter in the data at higher J values and in $v = 1$ is caused by diminished signal levels. The measured distributions are plotted in Figure 3, scaled to reflect the vibrational populations in $v = 0$ and $v = 1$. Boltzmann fits to the data are overlayed in the figure. It should be noted that the rotational temperature in $v = 1$ is more than twice that in $v = 0$.

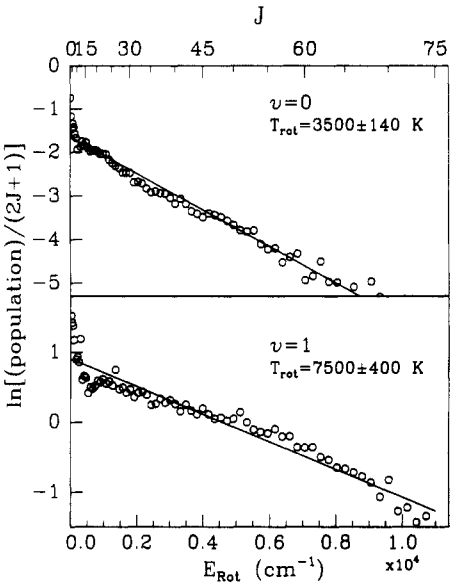

Figure 2. Boltzmann plots for the CO fragment rotational distributions in $v = 0$ and 1. The lines are least-squares fit to the data.

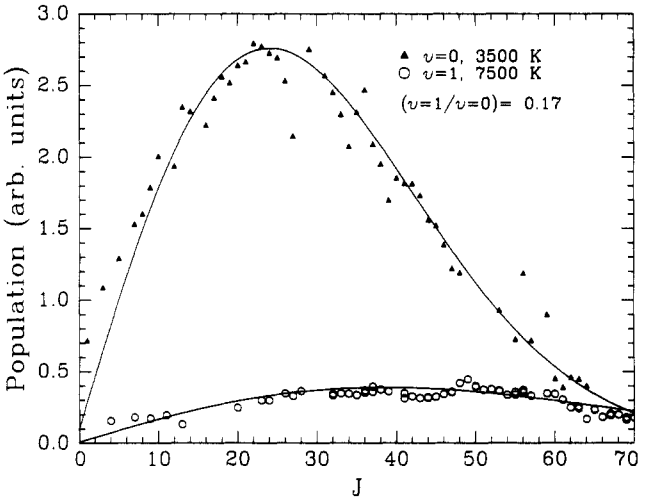

Figure 3. Rotational distributions of the CO photofragment in $v = 0$ and 1, scaled to reflect the relative populations in the two vibrational levels. For clarity, only the Q-branch data are shown.

(B) CO Vibrational Distribution. A measure of the relative CO vibrational populations in $v = 0$ and $v = 1$ was obtained by scaling the 0–1 band to the intensity of the 1–1 band, which overlapped the 0–0 band, and using the known Franck–Condon factors for each band.[20] The distributions were then integrated to the limit of available energy in each level, and after being divided by their respective Franck–Condon factors, the ratio of the two areas is the ratio of populations in the two vibrational levels. The ratio $v = 1/v = 0$ was found to be 0.17 ± 0.02. For a Boltzmann distribution, this ratio would correspond to a vibrational temperature of 1750 ± 200 K and to a prediction that approximately 3% of the population should be in $v = 2$. The prediction is consistent with the very small signal which we detected on the 0–2 band.

(C) CO Doppler Profiles. Doppler line shapes were recorded for several rovibronic transitions in both $v = 0$ and 1. The line shapes were seen to be nearly invariant with respect to vibrational level; lines of the same J in both levels were approximately the same. Doppler profiles of Q lines and the P or R lines of $v = 0$, $J = 20$, 30, 53, and 69 are shown in Figure 4. Two features of these Doppler profiles are noteworthy.

(18) Burak, I.; Hepburn, J. W.; Sivakumar, N.; Hall, G. E.; Chawla, G.; Houston, P. L. *J. Chem. Phys.* **1987**, *86*, 1258.

(19) LeFloch, A. C.; Launay, F.; Rostas, J.; Field, R. W.; Brown, C. M.; Yoshino, K. J. *J. Mol. Spectrosc.* **1987**, *121*, 337. Field, R. W. Unpublished results.

(20) Waller, I. M.; Hepburn, J. W. *J. Chem. Phys.* **1988**, *88*, 6658.

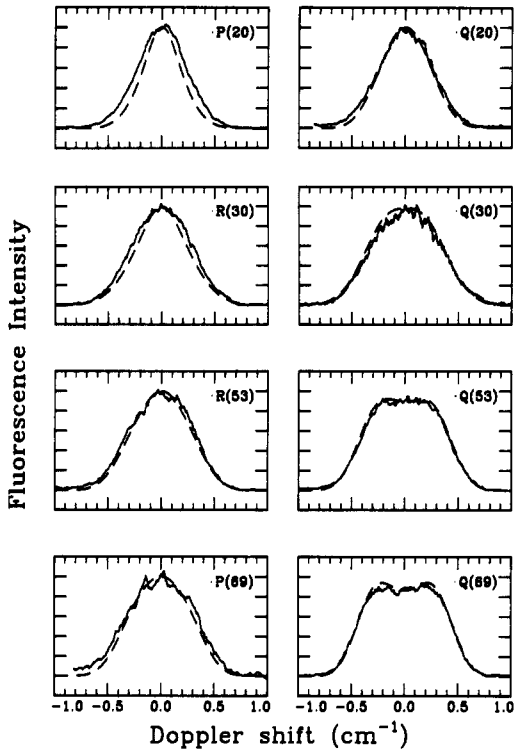

Figure 4. Doppler profiles of various CO fragment $v = 0$ rovibronic transitions. Each solid curve is the average of several measurements. The dashed lines are simulated Doppler profiles which are calculated from the translational energy distributions in Figure 5, with the assumption that $\mathbf{v} \perp \mathbf{J}$. The improved fits at higher J indicate the improvement of the vector correlation at these J values.

First, the Doppler profiles become wider with increasing J. This trend is seen in both $v = 0$ and 1 and established that CO fragments in higher rotational levels have a propensity to have more translational energy than those in lower rotational levels. The rate of increase in Doppler width slows for $J > 50$, and after $J \approx 60$ the profiles remain roughly constant. This limitation on the velocity does not stem from energy conservation and so must have some other cause. Neither trend is expected from a simple statistical model. We examine them more closely in the Discussion.

Second, the difference between the shapes of the P/R and Q lines establishes the presence of a vector correlation.[21] The correlation manifested in this case is a perpendicular alignment of the CO angular momentum vector with respect to the CO velocity vector ($\mathbf{v} \perp \mathbf{J}$). At low J values, however, the difference between the P/R and Q lines diminishes, to the point where P(20) is only slightly narrower than Q(20).

The Doppler line shapes were not affected by changing the angle between the direction of the linearly polarized dissociation light and the probe direction. The absence of an effect indicates either that the distribution of photofragments is isotropic in space or that they are produced at the magic angle. Since the latter situation is unlikely, the implication is that the dissociation is slow on the time scale of the parent molecule's rotational period, i.e., about 10^{-10} s.

The extraction of translational energy distributions from Doppler profiles is nontrivial in the presence of vector correlations. Three factors influence the shape of a Doppler profile: the translational energy distribution, the spatial distribution of recoil vectors in the laboratory frame (the μ–v correlation), and the distribution of angles between the rotation vector and the fragment recoil velocity vector (the v–J correlation). We have demonstrated that the distribution of recoil vectors in the laboratory frame is nearly isotropic, so the Doppler profiles of Figure 4 reflect jointly the distributions of v–J angles and translational energy. In theory, these distributions may be correlated, in which case extraction of speed and v–J angular distributions would be very difficult

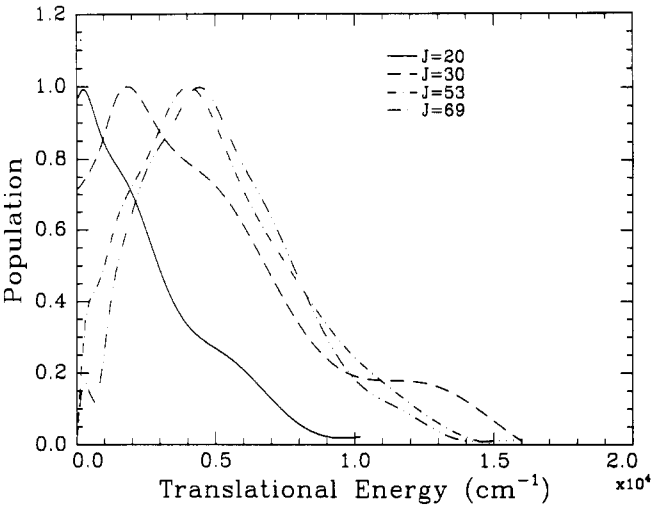

Figure 5. Translational energy distributions calculated from the Doppler lines in the previous figure. They are averages of a distribution calculated from a P or R line with that calculated from a Q-branch line.

TABLE I: Average Energies in Each Degree of Freedom of the CO Photoproduct after 193-nm Dissociation of 3-CPE and Comparison with the Statistical Prior Values

	data, cm^{-1}	prior, cm^{-1}
rotation		
$v = 0$	2400	2250
$v = 1$	5200	2170
translation ($v = 0$ and 1)		
$J = 20$	2500	3380
$J = 30$	4500	3330
$J = 53$	5000	3130
$J = 69$	5100	2920
vibration	540	1090

indeed. However, for the present case the v–J correlation appears unambiguously, and we have assumed that the v–J and translational energy distribution are uncorrelated, i.e., that the total distribution can be factored into the product of a translational energy distribution and a δ function distribution over v–J angles where v and J are perpendicular. Given this assumption, the method for extraction of the translational energy distribution is described in the appendix. The results for $v = 0$ are shown in Figure 5. Approximately the same distribution was obtained whether starting from the Q or P/R Doppler profiles, a fact which at least partially justifies the separability assumption.

(D) Summary of Data. Table I summarizes the average fragment energies measured in the experiment and also lists the average energies calculated using a simple prior (statistical) model described in the next section. The available energy of the reaction, E_{avail}, was taken to be 46 600 cm^{-1}. In the average dissociation, the CO fragment is found experimentally to receive about 5800 cm^{-1} of energy, while the butadiene by difference receives about 40 800 cm^{-1}.

Discussion

(A) A Reference Distribution: The Statistical Prior. Statistical prior distributions form a useful reference from which to measure deviations due to the detailed dissociation dynamics. Such distributions have been calculated by (1) treating CO rotations and vibrations quantum mechanically and using a direct count over the states, (2) calculating the butadiene vibrational density of states from the harmonic frequencies of *trans*-butadiene,[22] by use of the Whitten-Rabinovitch approximation,[23] and (3) assuming that every state of the products is equally likely. We compare below the resulting statistical distributions with those found experimentally.

1. Rotational Distribution. While the $v = 0$ rotational distribution is in reasonable agreement with the statistical prior

(21) Houston, P. L. *J. Phys. Chem.* **1987**, *91*, 5388.

(22) Harris, R. K. *Spectrochim. Acta* **1964**, *20*, 1129.
(23) Whitten, G. Z.; Rabinovitch, B. S. *J. Chem. Phys.* **1964**, *41*, 1883.

model, the $v = 1$ vibrational level is rotationally quite hot compared to the prior. The rotational surprisal plots[24] for both $v = 0$ and $v = 1$ are linear with slopes of $\theta = -1.7$ and $\theta = -12.0$, respectively, indicating that the rotational excitation for $v = 1$ is much higher with respect to the prior than for $v = 0$. This effect has been previously observed in the dissociations of acetaldehyde[25] and carbon suboxide[26] and to a lesser extent in the dissociation of acetone[27] and cyclobutanone.[28] The explanation previously put forth considered an analogy with the scattering of hot H atoms from CO.[29] It is found in these scattering experiments that H atoms stiking the CO in the region of the HCO well efficiently impart both vibrational and rotational energy to the CO. The well occurs at an HCO bond angle of 126°. The CO rotation occurs predominantly in the plane of the three atoms. In the 3-CPE dissociation, therefore, this explanation might also account for CO rotation. For a stepwise dissociation, the CO would then rotate in the plane containing the CO and the CC bond that breaks last. For a concerted dissociation, this mechanism for producing correlated rotational and vibrational excitation would require the CO bond to be located out of the plane of the cyclopentenone.

The value of 2890 ± 190 K for T_{rot} in $v = 0$ reported by Prather and Rosenfeld was obtained by extrapolating to zero time delay the rotational temperatures for a fixed starting pressure measured as a function of delay between photolysis and probe laser. CO rotational relaxation is very rapid, so that the measured rotational temperature falls from 2300 to 300 K for delays of 1–20 μs. Their error bars at the higher temperatures are appreciable, and a slightly different extrapolation leading to our directly measured value of 3500 ± 140 K would be quite reasonable.

Prather and Rosenfeld could not measure rotational energy distributions in states with $v > 0$ due to the limited signal-to-noise level. This failure is not surprising. Our result that $T_{rot}(v=1) = 7500 \pm 400$ K implies that the population is spread over many more rotational energy levels, so that any given rotational line will have relatively small intensity. Also, there is less population in higher vibrational levels, as discussed next.

2. Vibrational Distribution. The CO photoproduct with an observed $v = 1/v = 0$ ratio of 0.17 clearly indicates less vibrational excitation than expected on statistical grounds, where one would predict a ratio of 0.38 (the vibrational surprisal plot, based on these two ratios is, of course, linear and has a slope of 17.5). This general observation concerning the CO vibrational distribution has been made by other authors who studied both the thermal and photochemical dissociations.[10,14] It is known that the CO bond length in ground-state 3-cyclopentenone is 1.215 Å, whereas in free CO it is 1.1316 Å.[30,31] Since either a $\pi^* \leftarrow \pi$ or $\pi^* \leftarrow$ n transition would weaken the C–O bond, the likely absorptions would reach a state which has a CO bond length greater than or equal to that of the ground state and definitely greater than that of free CO. The fact that only little vibrational excitation is observed compared to the statistical prediction indicates that much of the CO bond change must occur before any impulsive release of energy, i.e., that the CO bond length at the transition state must be close to that of free CO.[3]

Prather and Rosenfeld report a vibrational temperature of 2900 ± 200 K at 193 nm, whereas we have measured a $v = 1/v = 0$ ratio which corresponds to a temperature of 1750 ± 200 K. While the reason for this difference is not known, it should be pointed out that when probing of only a few low-J rovibronic transitions is used to determine the vibrational distribution,[14] a small deviation in the rotational distribution can cause a relatively large error in the determination of vibrational population.[32]

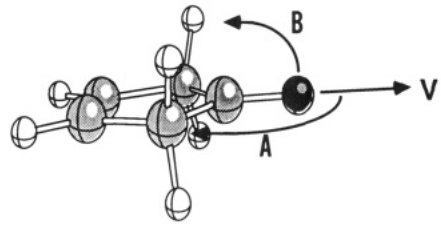

Figure 6. Two dissociative motions which may cause $\mathbf{v} \perp \mathbf{J}$. The CO velocity will always be away from the ring. If the molecule dissociates via an in-plane motion of the CO, as in case A, then **J** will be perpendicular to the ring plane. However, if the CO breaks away from the ring with the O moving perpendicular to the plane, as in case B, then **J** will lie in the ring plane.

3. Translational Energy Distribution. The translational energy distributions of the CO photoproducts are not well described by a statistical distribution for two reasons. First, the statistical distribution gives nearly a Boltzmann distribution of velocities for each rovibronic level, contrary to observation. Second, it predicts that CO fragments having more rotation and vibration will have less translational energy, since less energy is available for partitioning between butadiene vibration and product translation after energy is disposed into those two degrees of freedom. Exactly the opposite trend is observed for a range $J = 20$–69 in $v = 0$ and 1. The translational energy distributions show maxima that move to higher energies at higher J values (see Figure 5).

Prather and Rosenfeld measured a translational temperature for $v = 0$ and $J = 18$ of 2210 ± 210 K. Our translational energy distributions are not Maxwell–Boltzmann, but that for $v = 0$ and $J = 20$ corresponds to a temperature of approximately 1800 K, in qualitative agreement with their value.

4. Vector Correlations. CO photoproduct isotropy: Rosenfeld and co-workers[14] have suggested that following excitation at 193 nm, 3-CPE decays nonradiatively to the ground-state surface prior to dissociation. Our measured value of $\beta = 0$ supports this conjecture and further suggests that the crossing takes place more slowly than rotation of the parent molecule. The dynamics of electronically excited 3-CPE might thus be similar to those of other molecules undergoing ring opening. Mathies et al. have used absolute resonance Raman intensities and picosecond time-resolved resonance Raman spectroscopy to study the photochemical ring opening of 1,3-cyclohexadiene.[33] Absolute resonance Raman intensities indicate rapid (10 fs) depopulation of the initially excited state into another electronically excited state. The picosecond measurements reveal a product formation time of 8 ± 1 ps. These authors explain the time lag between the initial depopulation and the product appearance as that required for crossing to the ground electronic state, whereupon dissociation occurs rapidly.

v–J correlations: Since the statistical distribution assumes that every state of the products is equally likely, we should not expect on statistical grounds to find correlations between, say, the relative recoil velocity vector **v** and the CO rotation vector **J**, but a strong correlation with $\mathbf{v} \perp \mathbf{J}$ is observed. As shown below, this vector correlation is an important indication that the reaction occurs by a concerted mechanism. Figure 6 shows two limiting dissociation pathways which start from a planar transition state geometry that are consistent with the $\mathbf{v} \perp \mathbf{J}$ observation. In one case (A of Figure 6), the CO rotation vector is perpendicular to the plane of the ring, and its velocity vector is located in the plane of the ring and pointing away from the butadiene center of mass, as required by conservation of linear momentum. Clearly **v** and **J** would be perpendicular for this limiting dissociation pathway. An alternative scenario (B of Figure 6) is that the CO undergoes a wagging motion perpendicular to the plane of the ring and that it dissociates via a repulsive force that imparts rotation. Again, **J** would be

(24) Levine, R. D.; Bernstein, R. B. *Molecular Reaction Dynamics and Chemical Reactivity*; Oxford University Press: Oxford, 1987; section 5.5.
(25) Kable, S. H.; Loison, J.-C.; Houston, P. L., unpublished results.
(26) Strauss, C. E. M.; Kable, S. H.; Chawla, G. K.; Houston, P. L.; Burak, I. *J. Chem. Phys.* **1991**, *94*, 1837–1849.
(27) Trentelman, K. A.; Kable, S. H.; Moss, D. B.; Houston, P. L. *J. Chem. Phys.* **1989**, *91*, 7498.
(28) Trentelman, K. A.; Kable, S. H.; Moss, D. B.; Houston, P. L. *J. Phys. Chem.* **1990**, *94*, 3031.
(29) Chawla, G. K.; McBane, G. C.; Houston, P. L.; Schatz, G. C. *J. Chem. Phys.* **1988**, *88*, 5481.
(30) Lewis, J. D.; Laane, J. *J. Mol. Spectrosc.* **1974**, *53*, 417.
(31) Herzberg, G.; Huber, K. P. *Constants of Diatomic Molecules*; Van Nostrand Reinhold: New York, 1979.
(32) Houston, P. L.; Moore, C. B. *J. Chem. Phys.* **1976**, *65*, 757.
(33) Reid, P. J.; Doig, S. J.; Mathies, R. A. *Chem. Phys. Lett.* **1989**, *156*, 163.

perpendicular to v, but in this case J would be parallel to the ring. Any motion which can be expressed as a linear combination of these two limiting motions will cause $v \perp J$, so it is perhaps not surprising that we have observed such a correlation. This vector correlation will be discussed in more detail below.

Prather and Rosenfeld, in their sub-Doppler measurements of the CO product rotational–vibrational spectra, found that the line shapes were Gaussian. In contrast to the CO LIF spectra, the Q-branch is forbidden in the IR spectra of CO. The observation of the vector correlation relies on the comparison between the Q-branch and P- or R-branch lines of the same rotational level. We find that up to $J = 30$ the P and R branch lines of our LIF spectra are fit well by Gaussian curves, with large deviation from Gaussian shape occurring only at very high J values ($J > 60$). Additionally, even one collision would serve to destroy the alignment between v and J found in the nascent CO product.

(B) Joint Probability Distribution. Since it is clear from the above that there are significant deviations between the measured distributions and the statistical distribution, it is pertinent to ask what is the distribution over all correlated variables which agrees with the data but otherwise makes no assumptions, i.e., is as uninformative (as close to the prior) as possible. Strauss, Jimenez, and Houston[34] have considered this problem and provided a numerical method for calculating what they call the joint probability distribution $P(E_v^a,E_r^a,E_t,E_v^b,E_r^b)$, based on an earlier paper.[35] This distribution gives the probability of observing simultaneously an energy E_v^a in the vibrational degree of the (diatomic) fragment a, of an energy E_r^a in the rotational degree of fragment a, an energy E_t in relative translation, etc. The key ideas in the method are (1) that the observed data are simply projections onto lower dimensions of the joint probability distribution, and (2) that the "best" (in the sense of being least informative) joint probability distribution which also agrees with the data is given by information theory.[36-48] An advantage of calculating the joint probability distribution is that it can be used to calculate many dynamical parameters that are not directly accessible to experiments. For example, Strauss et al. show that the distribution of impact parameters for the dissociation, $P(b)$, is a projection of the joint probability distribution.[34] The method calculates the most probable $P(b)$ distribution based both on whatever experimental data are available and also on the prior statistical information, including conservation of energy, linear momentum, and angular momentum. While the most probable $P(b)$ distribution is not necessarily the correct one, it is the best and least biased guess that can be made using only the information available.

(C) Inferences from the Joint Probability Distribution. *1. Is the Reaction Stepwise or Concerted?* Strauss et al. have shown that by comparing the $P(b)$ distribution consistent with the data

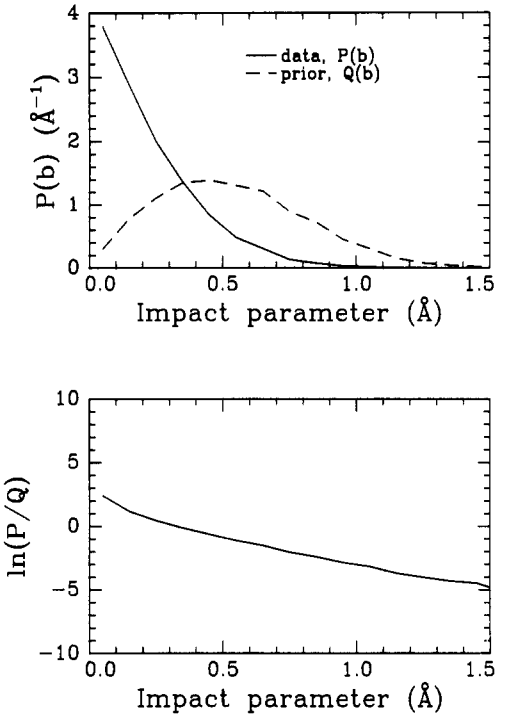

Figure 7. (a, top) Impact parameter distributions for 3-CPE calculated via the maximum entropy method. The distribution shown is for counterrotating photofragments. (b, bottom) Surprisal plot of the data shown in the top frame.

to that based on the prior information alone, it is possible to obtain a qualitative measure of the rigidity of the transition state.[34] The method was illustrated by using data from the photodissociation of formaldehyde to H_2 and CO.[49] The data used for formaldehyde were the translational energy distribution, the CO $v = 0$ and $v = 1$ rotational distributions, and the H_2 rotational distributions in $v = 0$, 1, 2, and 3. It was found that the $P(b)$ calculated by this method agreed closely with that calculated by Debarre et al.[49,50] The $P(b)$ distribution from the data is sharply peaked in comparison to that derived from the prior alone and can be interpreted as indicating that the dissociation takes place through a limited region of the statistically available phase space.

A calculation for the dissociation of 3-CPE was performed in a manner similar to that previously described for formaldehyde. A joint probability distribution was formed by using six projections: the $v = 0$ and 1 CO rotational distributions, and the translational energy distributions for CO(v=0) with $J = 20$, 30, 53, and 69. The experimentally measured distributions were binned into 100 element arrays, and the computation was performed on an IBM ES/3090-600J. It took approximately 15 min of CPU time to calculate the $P(b)$ distributions from a joint probability distribution that yields projections agreeing with the data. In calculating the impact parameter distribution, the butadiene was approximated as a diatomic rotating about the a axis with rotational constant approximated by the *trans*-butadiene constant of 1.37 cm^{-1} and rotational degeneracy $(2J + 1)$.[51] Choice of another rotational constant (e.g., that for *cis*-butadiene) or inclusion of K-state degeneracy would change both the calculated and prior $P(b)$ distributions but would not change the qualitative relationship between them. The vector correlation of $v \perp J$ was also included, with the assumption that the fragments are counterrotating. Counterrotation will result from the impulsive dissociation of a molecule if the line of impulse does not cross the line connecting the fragments' centers of mass. Corotation, while conceivable,

(34) Strauss, C. E. M.; Jimenez, R.; Houston, P. L. *J. Phys. Chem.*, in press.
(35) Strauss, C. E. M.; Houston, P. L. *J. Phys. Chem.* **1991**, *94*, 8751.
(36) Levine, R. D. *Annu. Rev. Phys. Chem.* **1978**, *29*, 59–92.
(37) Skilling, J. Classical Maximum Entropy. In *Maximum Entropy and Bayesian Methods*; Kluwer Academic: 1989; pp 42–52.
(38) Gull, S. F.; Skilling, J. The Maximum Entropy Method. In *Indirect Imaging*; Roberts, J. A., Ed.; Cambridge: London, 1984.
(39) Gull, S. F.; Skilling, J. *IEE Proc.* **1984**, *131*, 646.
(40) Rivier, N.; Engleman, R.; Levine, R. D. Constructing Priors in Maximum Entropy Methods. In *Maximum Entropy and Bayesian Methods*; Fougere, P. F., Ed.; Kluwer Academic: Dordrecht, Holland, 1990; p 233.
(41) Frieden, B. R. *Maximum Entropy and Bayesian Methods in Inverse Problems*; Smith, C. R., Grandy, W. T., Eds.; D. Reidel: Dordrecht, Holland, 1985; pp 133–169.
(42) Jaynes, E. T. *Maximum-Entropy and Bayesian Methods in Inverse Problems*; Smith, C. R., Grandy, W. T., Eds.; D. Reidel: Dordrecht, Holland, 1985; p 21.
(43) Grandy, W. T. *Maximum-Entropy and Bayesian Methods in Inverse Problems*; Smith, C. R., Grandy, W. T., Eds.; D. Reidel: Doredrecht, Holland, 1985; p 1.
(44) Jaynes, E. T. *Maximum Entropy Formalism*; MIT Press: Cambridge, MA, 1978; p 15.
(45) Shannon, C. E. *Bell System Tech. J.* **1948**, *27*, 379, 623.
(46) Levine, R. D. *Adv. Chem. Phys.* **1981**, *47*, 239.
(47) Levine, R. D. *Maximum Entropy Formalism*; MIT Press: Cambridge, MA, 1978; p 247.
(48) Bernstein, R. B.; Levine, R. D. *Adv. At. Mol. Phys.* **1975**, *11*, 215.
(49) Debarre, D.; Lefebvre, M.; Péalat, M.; Taran, J.-P. E.; Bamford, D. J.; Moore, C. B. *J. Chem. Phys.* **1985**, *82*, 3032.
(50) Debarre et al. calculated $P(b)$ by making the assumption that the internal energy levels of H_2 and CO are uncorrelated. This assumption is reasonable but not rigorously justifiable.
(51) Herzberg, G. *Electronic Spectra of Polyatomic Molecules*; Van Norstrand Reinhold: New York, 1950.

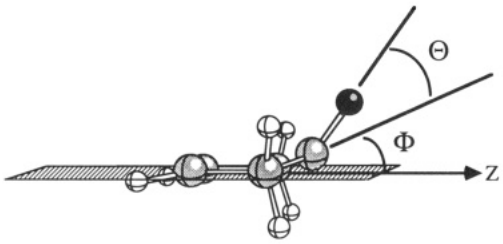

Figure 8. Geometric parameters of 3-CPE relevant to the interpretation of the impact parameter distribution.

can occur only for a few very restricted geometries.

The $P(b)$ distribution calculated from the method, along with the $P(b)$ distribution calculated from the prior distribution, are shown in Figure 7a. As can be seen from the figure, the experimental distribution of impact parameters is much narrower than the statistically available distribution of impact parameters, an observation which suggests a constrained transition state.

A physical interpretation of the $P(b)$ distribution for the dissociation of 3-CPE can be made by considering the $P(b)$ distribution that would result from a stepwise vs concerted reaction. In the stepwise case, which might involve for example a long-lived biradical intermediate, one bond breaks first, the intermediate species is then free to rotate internally for some time, and finally the second bond breaks, releasing CO and butadiene. The $P(b)$ distribution resulting from this sequence of events should be quite broad, since the unconstrained system would occupy nearly as much of phase space as available consistent with the conservation laws. Thus, the $P(b)$ distribution calculated from the data would not be expected to deviate significantly from that calculated from the prior alone.

Now consider the $P(b)$ distribution which would result from a concerted reaction; CO would be expelled from a ring which is nearly closed. For this case, we expect $P(b)$ to be quite narrow in comparison with the statistically available range of impact parameters. The impact parameter distribution would reflect both the conformation of the ring and the distribution of CO out-of-plane angles, as shown in Figure 8. Let R be the distance from the C atom in CO to the CO center of mass, let Θ be the CO out-of-plane angle, and let Φ be the angle between the plane formed by the α and β carbon atoms of the ring and the plane formed by the α carbons and the carbon atom of the CO. In the simplest case, assume that the only contribution to $P(b)$ comes from the CO out-of-plane wag. Then $\Phi = 0$ and $b(\Theta) = R \sin \Theta$, so that the maximum impact parameter could be $b = R = 0.65$ Å. From the $P(b)$ distribution of Figure 7a we find that the average value of $\sin \Theta$ is about $\Theta = 20°$ and that over 90% of the dissociations have less than the maximum impact parameter suggested by this simple model. Of course, the ring may be in a nonplanar conformation at the transition state so that $\Phi \neq 0$ and the impact parameter would increase. Either case would be expected to produce the observed $\mathbf{v} \perp \mathbf{J}$ correlation with the CO **J** vector parallel to the plane of the ring, as illustrated in case B of Figure 6.

A surprisal plot[52] of the $P(b)$ distribution is displayed in Figure 7b. Note that the plot is quite linear with a slope indicating a surprisal of 4.62. The fact that the curve is linear suggests that only one constrained controls the $P(b)$ distribution. This latter observation is consistent with the explanation that a distribution of CO out-of-plane bond angles is responsible for the $P(b)$ distribution.

Of course, it is quite possible that the experimental data obtained in our experiments do not form a sufficiently complete set of projections for determination of the actual $P(b)$ distribution. The maximum entropy method cannot guarantee that the $P(b)$ we have calculated is the actual distribution, merely that it is the least biased guess given the accumulated data. However, the addition of new data can only make the $P(b)$ distribution less

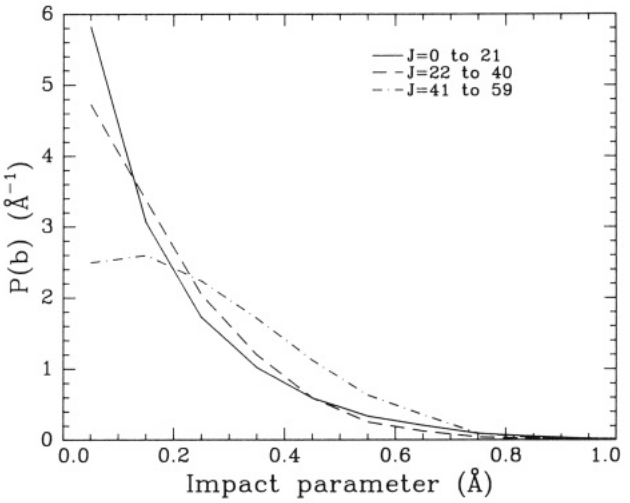

Figure 9. Impact parameter distributions for various ranges of J. They are scaled to reflect their relative populations.

statistical than that already calculated. We would certainly be more confident of our conclusion if the data included measurements on the butadiene fragment, and these may be necessary. On the other hand, the calculations on formaldehyde seem to indicate that the CO internal and translational energy distributions may be sufficient. For formaldehyde, measurements of either the rotational distributions from both fragments or the rotational and translational distributions from the CO fragment were sufficient to give a reasonably accurate $P(b)$ distribution. Since the latter set of distributions was used for 3-CPE, we are encouraged that the calculated $P(b)$ distribution will be an accurate reflection of the dynamics. It is important to note that inclusion of the observed **v**–**J** correlation makes a great deal of difference in the calculation; if the correlation is not included in the calculation, the resulting $P(b)$ does not differ significantly from the statistical distribution.

Clearly, the comparison of the $P(b)$ distribution to that from the prior serves as a measure of concertedness in this dissociation. A sharply peaked $P(b)$ indicates a concerted reaction, and a nearly statistical $P(b)$ indicates a stepwise process. On this basis, we suggest that the dissociation occurs via a concerted mechanism.

2. Why Does Translation Increase with Rotation? A surprising result of our investigation is that over the range up to $J \approx 60$, the Doppler profiles actually increase in width with increasing rotational energy, a observation which indicates that the CO velocity increases with increasing CO rotation. Energy conservation arguments might predict the opposite trend, but the energy available to the products is large compared to the translational or rotational energies of the CO. The phenomenon of Doppler profiles which do not decrease in width with increasing rotational quantum number has previously been reported twice. In the dissociation of *trans*-glyoxal,[53] the Doppler profiles broaden with J, whereas in the 157-nm photodissociation of carbon suboxide,[54] the widths of the Doppler profiles are the same for all CO rovibronic levels.

The cause of the increase in CO velocity with rotational level can be understood by considering conservation of angular momentum, which requires that

$$\mathbf{J}_{BDE} + \mathbf{J}_{CO} + \mu v b = \mathbf{J}_{3\text{-CPE}} \qquad (1)$$

where $\mathbf{J}_{BDE}$ is butadiene rotation, $\mathbf{J}_{CO}$ is CO rotation, μ is the reduced mass of the butadiene–CO system, v is their relative velocity, b is the impact parameter, and $\mathbf{J}_{3\text{-CPE}}$ is the parent molecule's rotation. The cyclopentenone in our experiment is dissociated in a supersonic expansion, so that we expect $\mathbf{J}_{3\text{-CPE}}$ to be quite low. Suppose further that $\mathbf{J}_{BDE}$ is also small. Conservation would then require (i) that $\mathbf{J}_{CO}$ and $\mu v b$ be oppositely directed

(52) Levine, R. D.; Ben-Shaul, A. In *Chemical and Biochemical Applicationsof Lasers*; Moore, C. B., Ed.; Academic Press: New York, 1977.

(53) Burak, I.; Hepburn, J. W.; Sivakumar, N.; Hall, G. E.; Chawla, G.; Houston, P. L. *J. Chem. Phys.* **1987**, *86*, 1258.

(54) Strauss, C. E. M.; Kable, S. H.; Chawla, G. K.; Houston, P. L.; Burak, I. R. *J. Chem. Phys.* **1991**, *94*, 1837.

(55) Gordon, R. D.; Orr, D. R. *J. Mol. Spectrosc.* **1988**, *129*, 24.

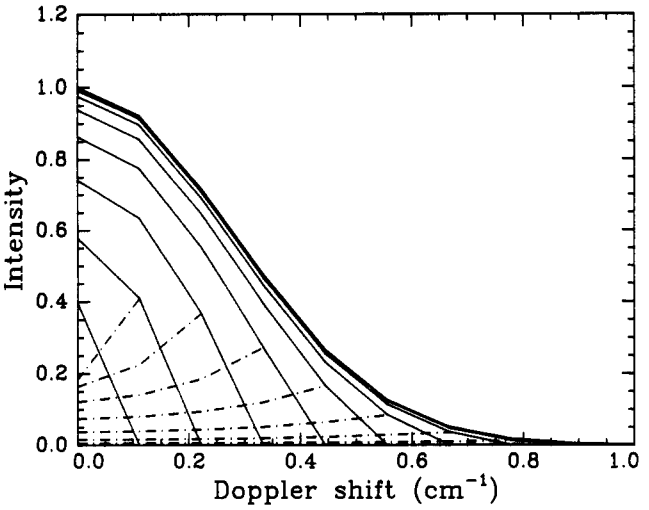

Figure 10. Doppler line (solid lines), $D(v)$ (dash–dotted lines), and several stages of decomposition of the Doppler profile. Only the right half of the Doppler profile is shown.

and (ii) that, for any fixed value of b, v must increase with J_{CO}. If the b and its range are constrained to be small by the dissociation, as appears to be the case from Figure 7a, then we might expect J_{CO} to increase with v, as observed. As a check on this hypothesis, we can examine the calculated $P(b)$ distribution for various ranges of J. As shown in Figure 9, this distribution does not change appreciably with J. The interpretation then suggests that J_{BDE} is small.

This point of view also explains why the Doppler profiles do not indefinitely broaden as J increases but rather reach a limit near $J \approx 60$. We have noted earlier that this limit is not an energy constraint. Geometrically, it seems reasonable to suspect that there is a maximum impact parameter which is reached at high J values, and from eq 1 and the previous approximations, that this impact parameter limits the velocity. The maximum impact parameter is likely to stem from a maximum bond angle allowed in the transition state. For example, suppose that the impact parameter were a result of the CO out-of-plane wag, as described above. The impact parameter would then vary with sin Θ, where the maximum angle for the wag is 90°. The limitation on the bond angle and its consequent limitation of the maximum impact parameter can therefore be viewed as the limit on the velocity.

Summary: Model for the Dissociation of 3-Cyclopentenone

The following picture of the photodissociation dynamics of 3-cyclopentenone emerges from the preceding discussion:

3-CPE absorbs a 193-nm photon, which excites a $\pi \leftarrow \pi^*$ transition.

There is a delay between the absorption of the photon and dissociation, which is due to the time required for the level crossing to the ground state. 3-CPE dissociates in concerted fashion, on the ground-state surface.

The dissociation occurs in a manner such that the CO is produced with J parallel to the plane of the ring.

The transition state for the reaction is fixed, and a maximum bond angle constraint limits the available range of impact parameters. This limitation accounts for the observed increase in translation with rotation.

Acknowledgment. The work at Cornell was supported by the National Science Foundation under grant CHE-8920404 and by a grant from the Cornell National Supercomputer Facility. We thank Professor Barry Carpenter for his comments and Professor James Burlitch for preparing a sample of 3-cyclopentenone, assisted by C.J.S.M.S. The work at Würzburg was financed by the Deutsche Forschungsgemeinschaft and Fonds der Chemischen Industrie.

Appendix: Calculation of Translational Energy Distributions from Doppler Profiles in the Presence of Vector Correlations

Define $D(v)$ to be the functional form of the Doppler curve for an ensemble of molecules all moving at a single speed. In the case of an isotropic distribution of velocities, with no vector correlations, moving at speed v, $D(v)$ is simply a constant, with edges that drop sharply at frequency

$$v = v_0[1 \bullet (v/c)] \tag{A.1}$$

For a distribution of speeds, we have a weighted sum over the $D(v)$ corresponding to all the speeds in the system. The weighting of each $D(v)$ in this sum gives the relative population at that speed. The experimentally observed Doppler line shape is the convolution of the laser line with this summed Doppler curve. In the simplest case, the experimentally observed Doppler profile from an ensemble of molecules with a Maxwell–Boltzmann distribution of speeds is simply a Gaussian line shape. The key to unravelling the speed distribution and thus the translational energy distribution from a Doppler profile, is to know the form of the single-speed Doppler profile, $D(v)$, as well as the width of the laser line, which is assumed here to be a Gaussian.

When vector correlations are present, such as spatial anisotropy of the fragments or alignment between v and J, the form of $D(v)$ is more complicated. The expressions for $D(v)$ when probing molecules with an isotropic distribution of velocities using LIF with polarized probe light and various detection geometries, with $v \perp J$ or $v \parallel J$, and using either Q or P/R transitions are given in Table II of ref 21. These expressions are given in terms of the cos χ, the projection of velocity on the probe axis, where χ varies from 0 at the maximally Doppler shifted frequency of $D(v)$ to $\chi = \pi/2$ at the center of the profile. To convert these expressions to $D(v)$, simply substitute $\chi = \cos^{-1}(v/v_{max})$, where v_{max} is the Doppler shift caused by a particular speed v, as given in eq A.1. Fragments whose velocities have zero projection on the probe axis exhibit no Doppler shift.

These $D(v)$ functions must be subtracted from the Doppler line in such a way that the highest speed $D(v)$ are subtracted first (since the wings of the Doppler profile have only contribution from the high-speed $D(v)$, while the center of the Doppler profile contains contributions from all $D(v)$). The subtraction proceeds from high speeds (wings) toward low speeds (center). At each step, the $D(v)$ function is scaled to match the maximally shifted edge of the remaining profile, and the height of the matching $D(v)$ curve is proportional to the population. Figure 10 shows a partially decomposed Doppler profile, which exhibits several $D(v)$ curves overlain on top of the original data, and the result of successive subtractions. In practice, about 150 subtractions yield a reasonable translational energy distribution.